

## Kastro Kokkinas

### Archaeological Background

Potsherds and other finds dated to the Neolithic Period, together with evidence of later habitation, were recently found on the natural hill called “Kastro” near the village of Kokkina. The location of the site is extremely interesting because it is located at the east entrance to a small and narrow flat pass that leads through the low hills of the area to the south-western part of the plain of Larissa.

References do not mention the exact phase of the Neolithic Period when the habitation first appeared there. However, according to our initial examination of surface material, the Late or Final Neolithic Period can be suggested at this point.

### Remotely Piloted Aircraft Systems (RPAS) Survey

Multiple orthophotos and digital elevation models have been produced for the site of Kastro Kokkinas, both in regular color and in the near-infrared bands. Some parts of the mosaics resulted in being slightly blurry because of the weather conditions at the time of the survey.

The close look and detailed examination of the images did not produce evidence of possible vegetation stresses with potential archaeological significance. This is probably due to the diffuse presence of rock outcrops and clearance areas, such that if something was actually there, it has most probably been destroyed by agriculture-related activities.

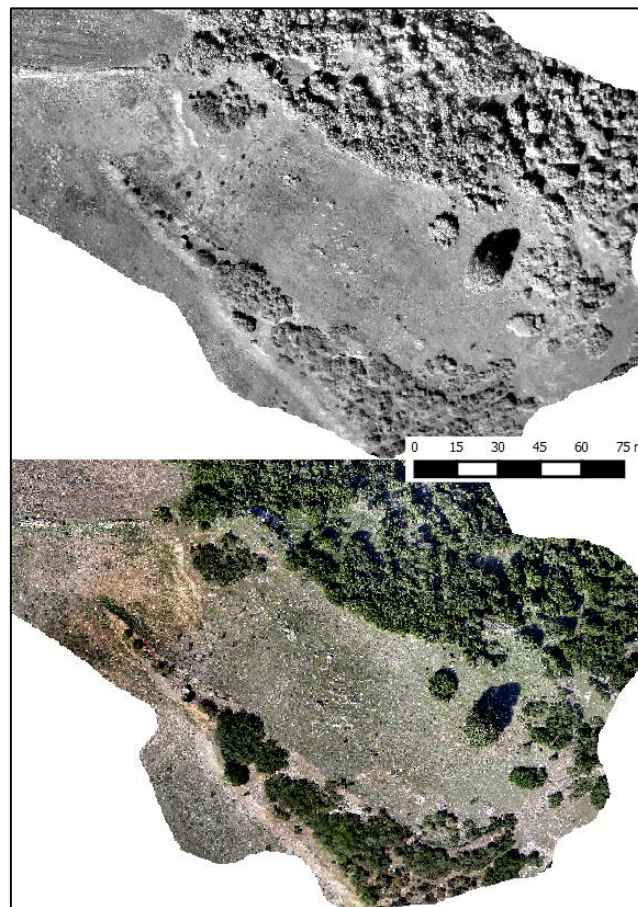


Figure 1: Kastro Kokkinas. Near Infrared (top) and regular RGB (bottom) orthophotos of the investigated site.

## Geophysical Prospection

### *Geomagnetic Survey*

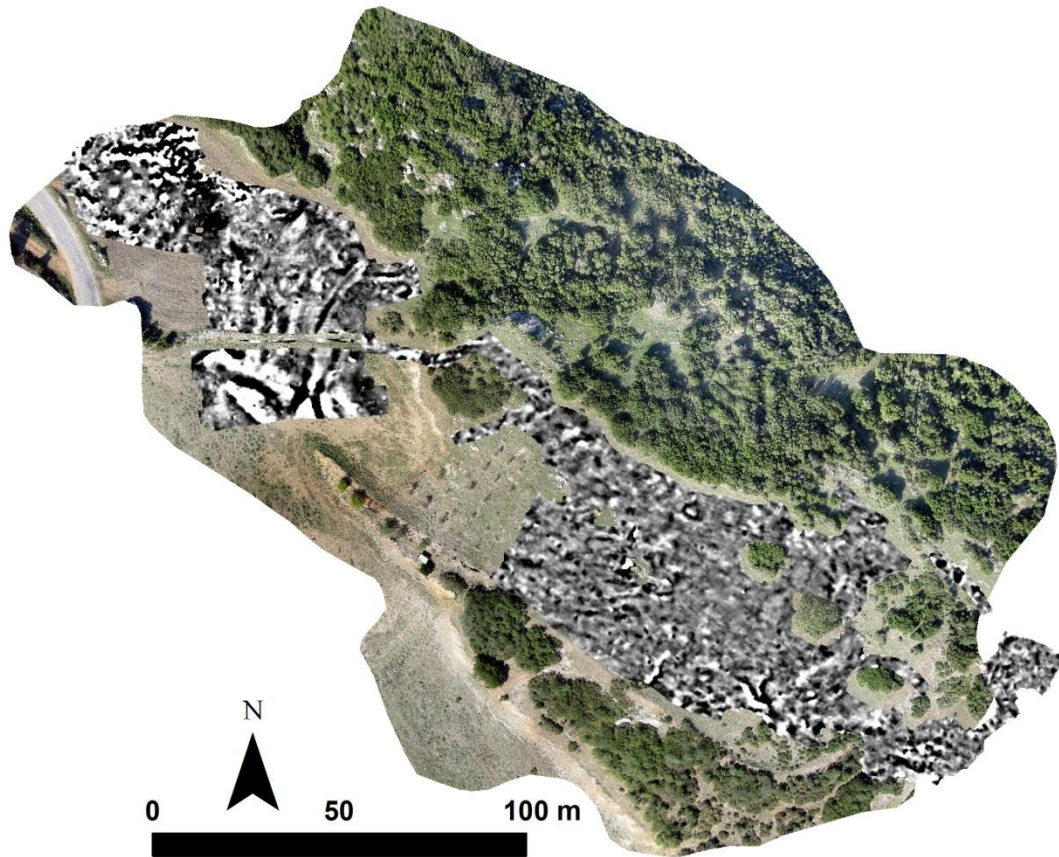


Figure 2: Results of the geomagnetic survey at Kastro Kokkinas

Patchy coverage of geomagnetic survey at Kastro Kokkinas leaves little room for accurate interpretation. Furthermore, the heterogeneity of the dataset makes anomaly-detection a challenging endeavor. Nevertheless, some interpretations can be suggested for the natural background. In the westernmost corner, a complex dipolar area is immediately visible. Considering its size and layout, the magnetic field generation is due to underlying bedrock.

Another set of low-high magnetic anomalies is detected further east. The north-south oriented dipolar anomaly bends towards the east and then towards the north and then abruptly stops. Curiously, the shape of this anomaly also does not fit with the local topography of the area (based on the DEM obtained from RPAS), so it remains undetermined. The same anomaly bifurcates towards the east and west in the south. These parts are better aligned with the local topography, such that it can be suggested that the anomaly is of geological origins, despite the potential counter-evidence in the north. Similar dipoles are also observed at the southeast boundaries of the survey area and also align with the digital elevation model.

### *Electromagnetic Induction Survey*

EM survey was conducted with the GEM2 from Geophex using 5 frequencies. We did a profile every 1 m with a GPS positioning. Data acquisition was done on top of the hill and in small open areas on the eastern slope. The data were processed in order to map the electrical conductivity, the magnetic susceptibility, and the magnetic viscosity extracted from the two lowest frequencies.

The electrical conductivity is very low: between 12 and 18 mS/m (Figure 3). This low value can explain the noisy results—we reached the limit of sensibility of the EM device for measuring the electrical conductivity. The map does not show any archaeological evidence, only some global variation which is related to the geological background, with a low conductivity on top of the hill and the highest conductivity on the slope.

The magnetic susceptibility is clearer, but it does not reveal any archaeological remains (Figure 4). The same global variation is present on this map. In this case, where the geological background is very close to the ground surface, the EM seems to be a poor value for the archaeological characterization. Also, the magnetic susceptibility does not seem very clear in this context, and it is very hypothetical to say whether it comes from the lack of archaeological features or from the soil distribution.

The magnetic viscosity (Figure 5) does not present as clear results as the electrical conductivity. The value is relatively high, but this could correspond to a bad calibration. Nevertheless, the range is ca. 10% of the magnetic susceptibility according to the theory. The magnetic viscosity does not reveal any archaeological features, only a low viscosity which seems to delimit the top part of the hill, with higher value on the slope.

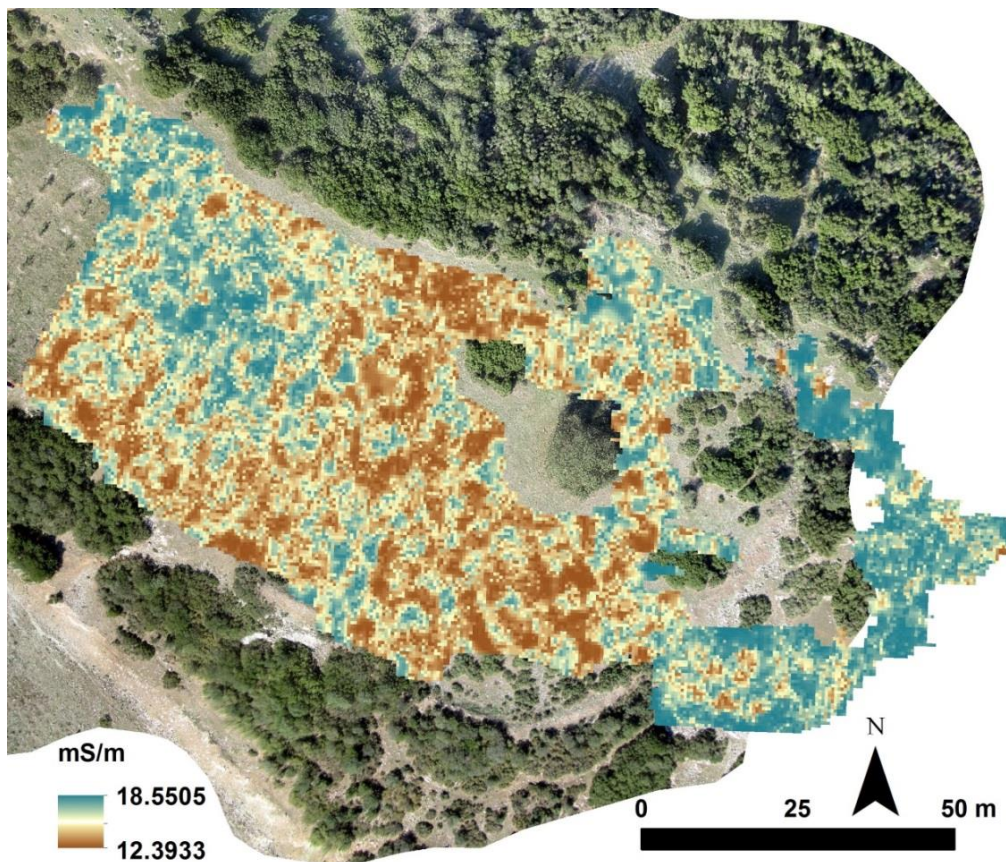


Figure 3: Georeferenced electrical conductivity at Kastro Kokkinas

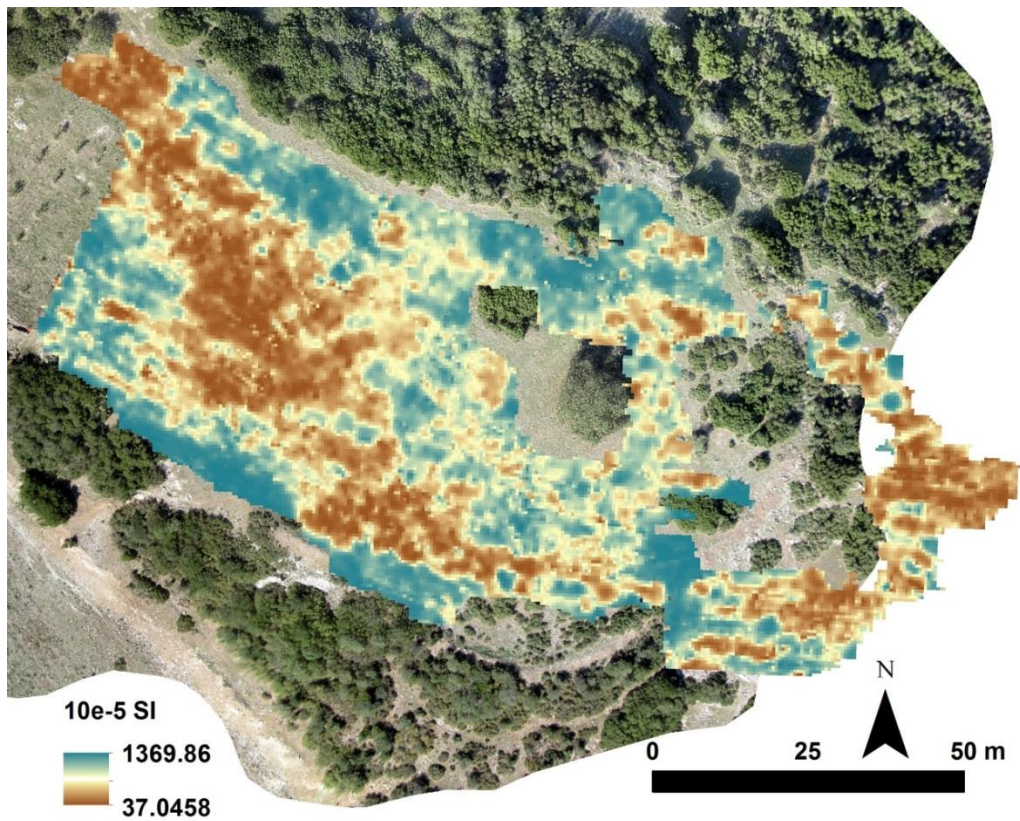


Figure 4: Georeferenced magnetic susceptibility at Kastro Kokkinas

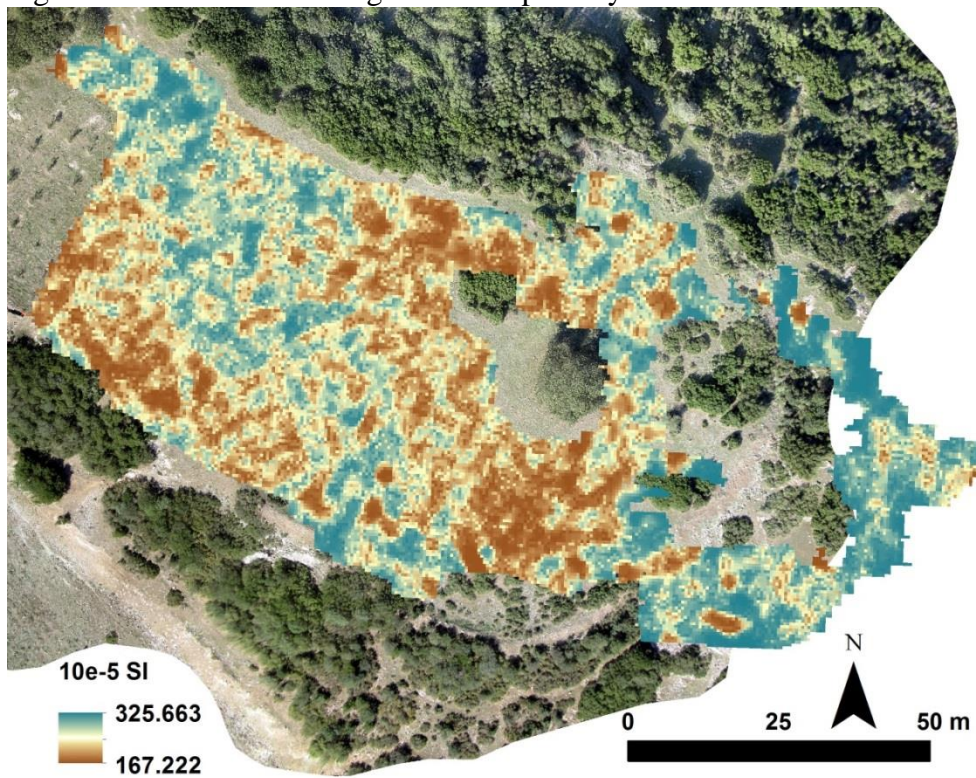
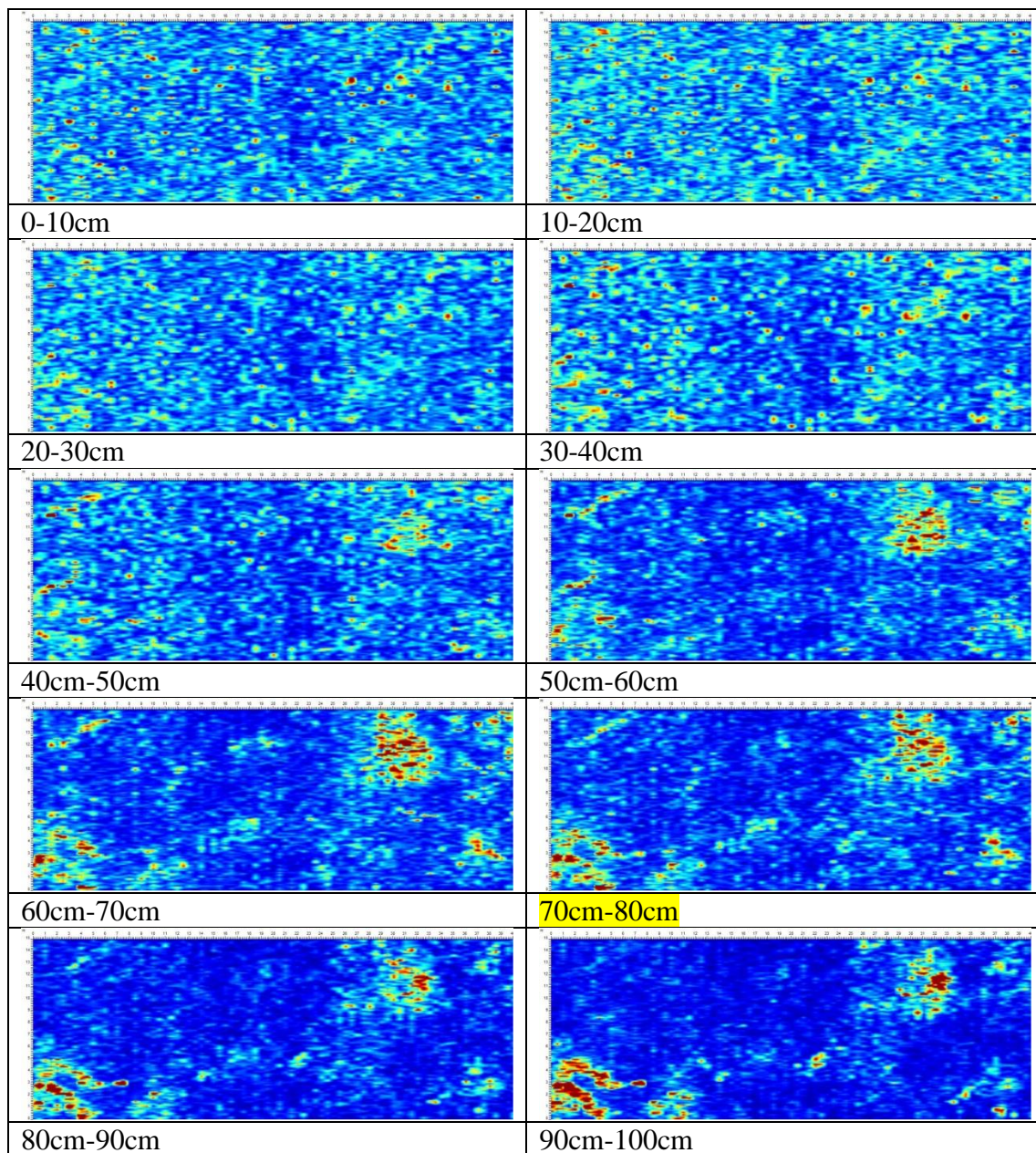


Figure 5: Georeferenced magnetic viscosity at Kastro Kokkinas

### Ground Penetrating Radar Survey

The GPR survey grid was set on the top of the natural hill, and the resulting slices are presented in Table 1. The total area covered is 600 m<sup>2</sup>, while the filters and corrections applied in the collected scans are: Trace reposition, Repick first break (10%), Dewow, SEC2 (Atn=17.69 dB\_m, StrtG=5.13,MaxG=367), Background average subtraction, Lowpass filter (f=50% Nyquist), Highpass filter (30% Nyquist).

The results within the range 0-50 cm exhibit small, scattered anomalies which are caused most probably by rocks. At deeper levels, a few stronger anomalies show up which outline reflectors of irregular shape. These reflectors are better shown in Figure 6, where different perspectives of the 3D GPR model are presented.



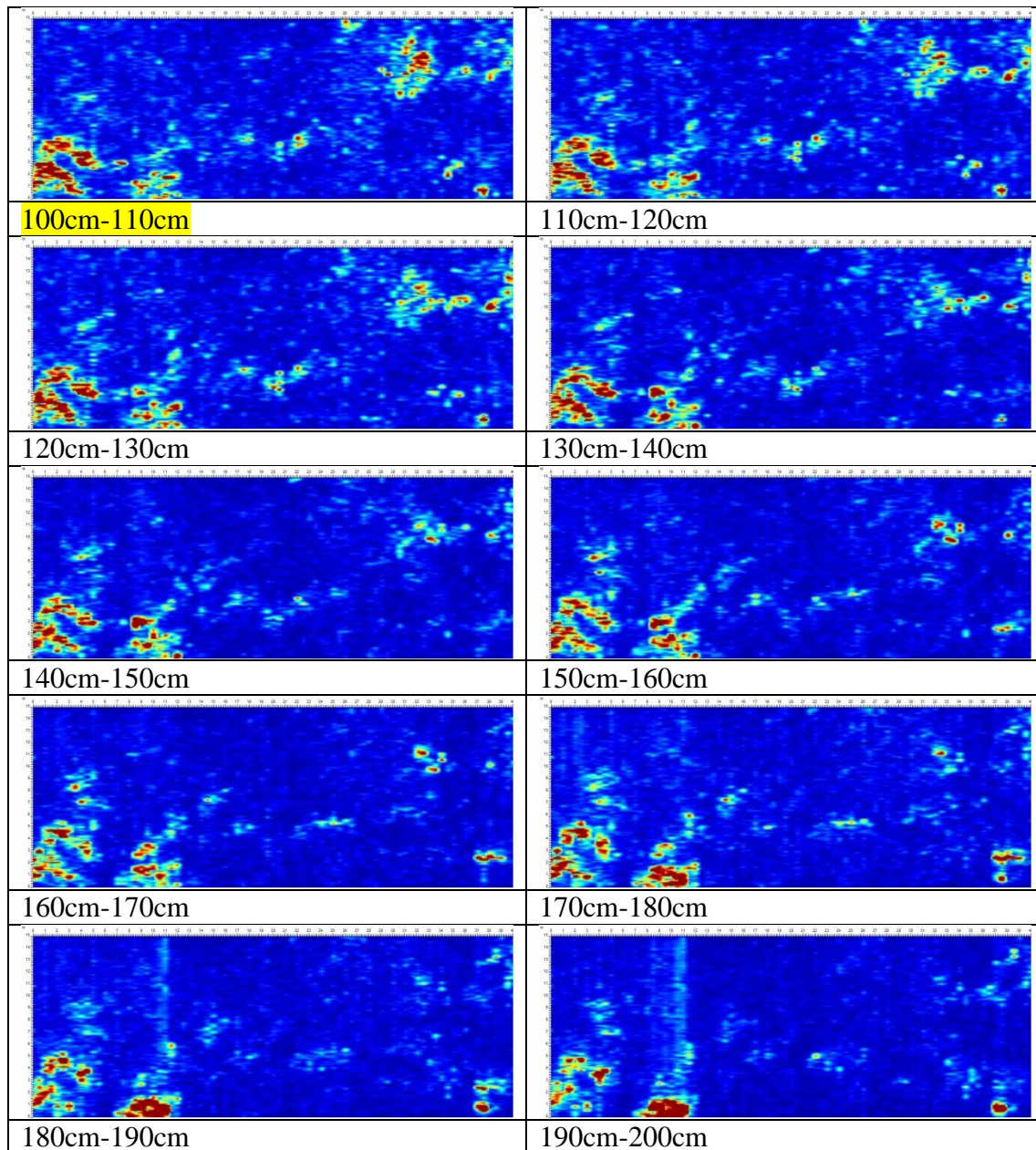


Table 1: GPR depth slices for the grid with code name KK1KK2 at Kastro Kokkinas with 10 cm thickness.

In Figure 7a, a representative GPR slice is presented describing the most important reflectors within the range 50-100 cm. The anomaly A1 (Figure 7b) presents linearity and extends from the northwest to southeast. It shows up from 50 to 80 cm. In contrast with the rest of the anomalies, A1 has weaker amplitudes. The anomaly A2 (Figures 7 and 8) first appears at 60 cm as small area of scatters with strong response; but as it extends deeper, its shape and limits become clearer. The anomaly A2 seems to extend below 200 cm, presenting at the same time very strong amplitudes and it could be assigned to bedrock. Similar to A2 is the reflector A3, which has a circular shape closer to the surface (50-80 cm), while it fades below 120 cm. It is not clear if the reflector in this case is due to the geomorphology of the area or to a demolished structure. A4 is an anomaly that appears from 50 to 80 cm. It presents strong amplitudes and could be related to the reflector A3, as they exhibit the same intensity in the

same depth range. Finally, the anomaly A5 (Figure 8b) shows up below 100 cm and seems to extend deeper than 200 cm, presenting at the same time very high amplitudes. It seems to be related to the reflector A2, and it is also identified as bedrock.

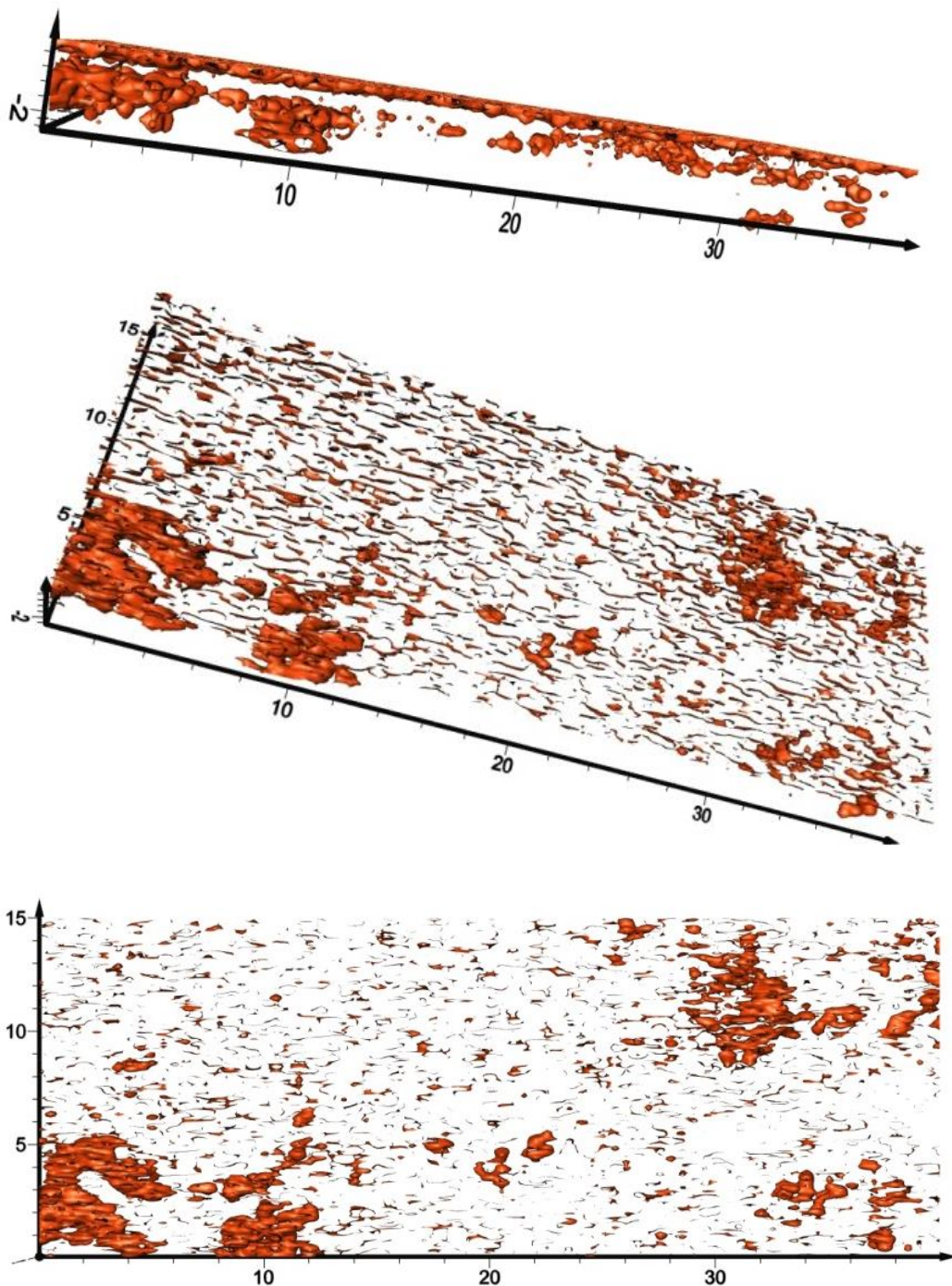


Figure 6: Different perspectives of the GPR 3D model describing the subsurface from the surface and up to 2.0 m depth.

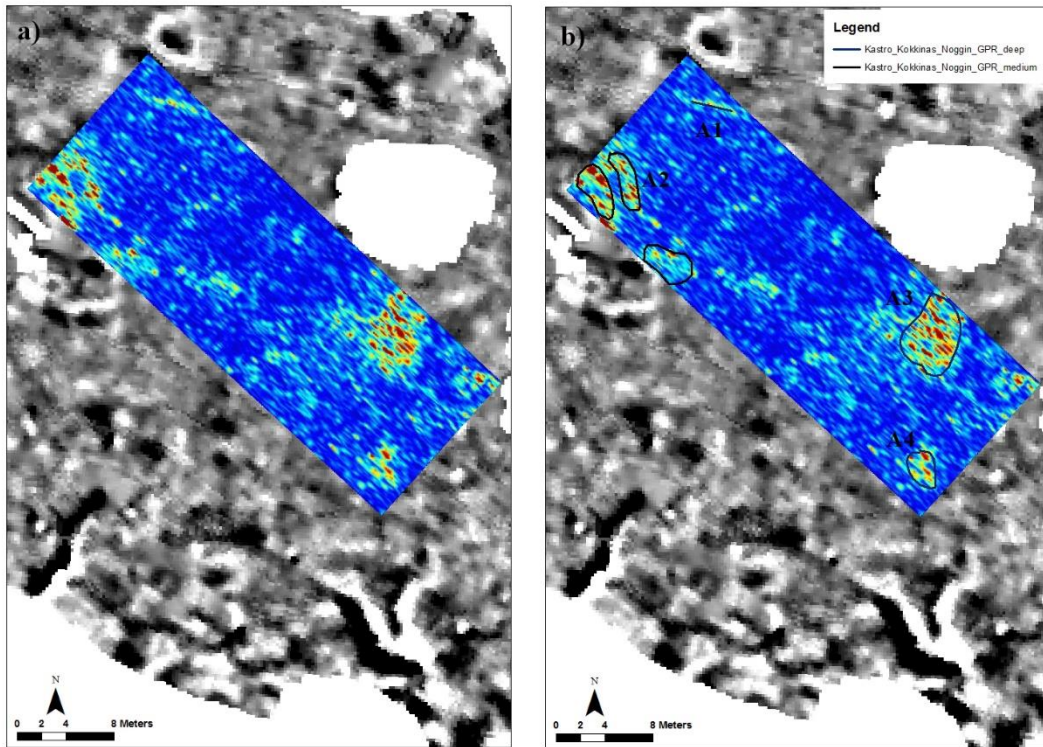


Figure 7: Georeferenced GPR slice at Kastro Kokkinas where a) the strongest anomalies at 70-80 cm depth are presented, while in b) the outline of each reflector is indicated.

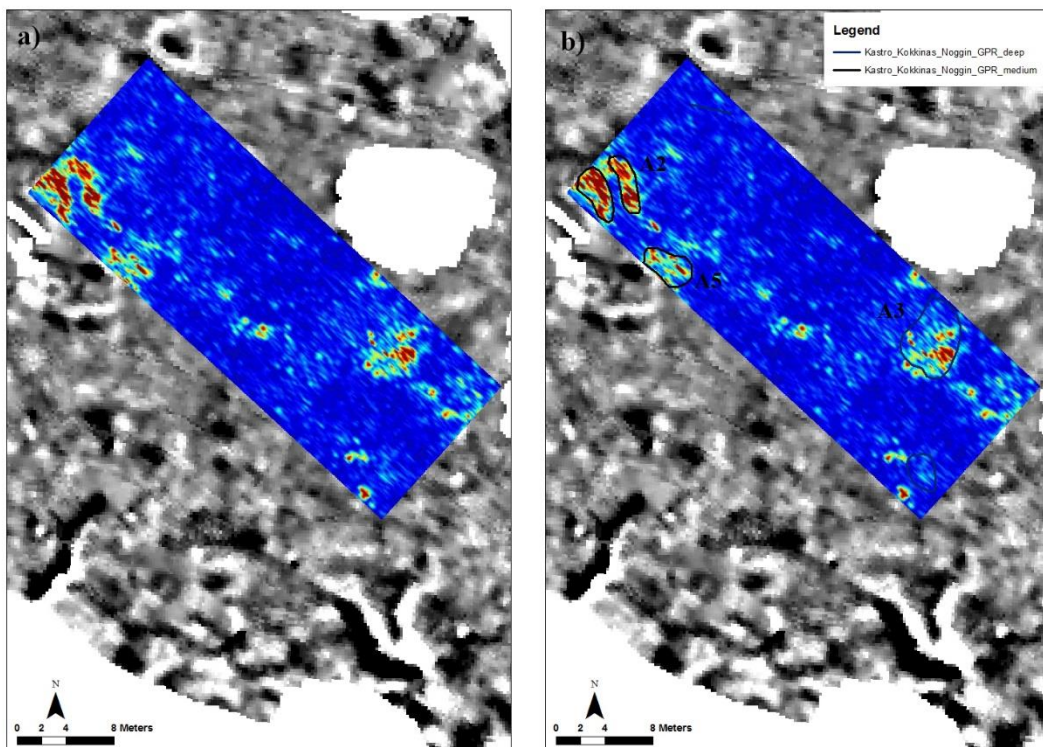


Figure 8: Georeferenced GPR slice at Kastro Kokkinas where a) the strongest anomalies at 100-110 cm depth are presented, while in b) the outline of each reflector is indicated.



The electrical sounding presents a two-layer model with resistive topsoil and a very high resistivity layer at 0.5 m, which corresponds to the geological background. This measurement and the electrical model explain the lack of resolution of the EM measurements at this site.

### *Site Bibliography*

Βουζαξάκης Κ., 2009. *Νεολιθικές θέσεις στη Μαγνησία. Ανασκόπηση – Ανασύνθεση δεδομένων*, στο Αρχαιολογικό Έργο Θεσσαλίας και Στερεάς Ελλάδας 2 (2006), τ. Ι, σελ. 61-74.

Ιντζεσίλογλου Α., 1995. *Επιφανειακές έρευνες, Νομός Μαγνησίας*, ΑΔ 44 (1989), Χρονικά, 228-229